# Influence of Fronts on the Spatial Distribution of Albacore Tuna (*Thunnus alalunga*) in the Northeast Pacific over the past 30 years (1982-2011)

Yi Xu[a], Karen Nieto[a,b], Steven L. H. Teo[a], Sam McClatchie[a], and John Holmes[c]

[a] Southwest Fisheries Science Center, National Marine Fisheries Service, NOAA

8901 La Jolla Shores Drive, La Jolla, California, 92037

[b] European Commission, Joint Research Centre, Institute for Environment and Substainability

Via E.Fermi, 2749, 21027, Ispra, VA, Italy

[c] Pacific Biological Station, Department of Fisheries and Oceans Canada

3190 Hammond Bay Road, Nanaimo, BC, Canada V9T 6N7

Corresponding author: Yi Xu Tel: 858-546-7074

Email address: Yi.Xu@noaa.gov

Abstract

The association of albacore tuna distribution with subtropical fronts in the Northeast Pacific was examined on seasonal and interannual scales from 1982 to 2011. Spatial analyses were performed on commercial logbook data from US and Canadian troll and pole-and-line fisheries targeting albacore tuna that were matched with corresponding satellite images from the Advanced Very High Resolution Radiometer (AVHRR). Subtropical fronts were detected by deriving sea surface temperature (SST) gradients on large basin-scales and by using an improved version of the Cayula-Cornillon frontal detection algorithm. Based on our results, we suggest that areas with high albacore catch-per-unit-effort (CPUE) tend to occur in regions with high SST gradients, such as the North Pacific Transition Zone (NPTZ) and the North American coast. Approaching the North American coast along the NPTZ, SST gradients drop off substantially around 130°W before increasing rapidly near the coast, which corresponded to a similar pattern in albacore CPUE. In the NPTZ, the centroid of albacore CPUE showed a seasonal shift northwards in summer and southwards in fall, which coincided with seasonal spatial shifts of areas with high SST gradients. A similar pattern was found on an interannual scale, with the exception of several years with limited fishery data in the NPTZ due to changes in fishery operations. A fine-scale analysis of frontal locations suggested that areas with high albacore CPUE are associated with oceanic fronts, with the highest albacore CPUEs observed within 100 km of the nearest front. In addition, albacore distribution is related to frontal strength, with the highest CPUE found near fronts with high SST gradient values in the range of 0.12-0.16°C $km^{-1}$. Integrating our findings on the influence of frontal areas on albacore distribution and abundance in the NEPO should improve the standardization model used to derive abundance indices for North Pacific albacore stock assessments.

INTRODUCTION

Albacore tuna (*Thunnus alalunga*) is a highly migratory species that is found primarily in the subtropical and temperate waters of the world's oceans, and is the target of numerous highly valuable fisheries. In the northeastern Pacific Ocean (NEPO), the north Pacific albacore troll and pole-and-line fisheries (surface fisheries) are the most important highly migratory species fisheries for both the U.S. and Canada. The combined albacore catch by U.S. and Canadian vessels in the surface fishery was more than 16,000 metric tons in 2012 (ISC, 2014). Historically, albacore were caught in both oceanic and coastal waters (Laurs and Lynn, 1977). In oceanic waters, albacore are primarily distributed from 30 to 45°N between the subtropical and subarctic fronts, along the North Pacific Transition Zone (NPTZ) (Shomura and Otsu, 1956; Graham, 1957; McGary et al., 1961). In coastal waters, the distribution spreads over a broader latitudinal band from 30 to 55°N, ranging from 50 to 350 km off the North American coast. During 1982-2011, albacore was heavily fished in coastal waters (Fig. 1), with relatively high catch-per-unit-effort (CPUE) of about 100 albacore per vessel per day (with a spatial resolution of 1x1 degree). In comparison, there are many "hot spots" in the offshore (west of 130°W) regions with CPUE as high as 200 albacore per vessel per day.

The general migration patterns of north Pacific albacore have been previously elucidated (Otsu and Uchida 1963; Ichinokawa et al. 2008), but the biological and environmental influences on these movements are still under investigation. Albacore in the north Pacific Ocean primarily spawn in the western and central Pacific Ocean and a portion of each cohort migrates from the western and central Pacific Ocean to the NEPO and are caught predominantly as 2 or 3 year old juveniles by the US and Canadian surface fisheries. These juvenile albacore arrive at the North American coast in summer and spend several months in coastal waters before heading back into oceanic waters in late fall (Clemens, 1961; Otsu and Uchida, 1963; Pearcy, 1973; Laurs and Lynn, 1977, and 1991; Ichinokawa et al. 2008; Childers et al. 2011).

Water temperature and food availability have been shown to influence albacore distribution in previous studies. Albacore abundance is highest in waters 16-19°C (Johnson, 1962; Laurs and Lynn, 1977) and aggregations are found in the eastern sector of the NPTZ concurrent with frontal structures during the early part of the fishing season (May-June) (Laurs and Lynn, 1991). By mid-July, some albacore migrate into coastal waters and appear to concentrate in the vicinity of cold, pigment-rich fronts related to coastal upwelling (Laurs and Lynn, 1977; Laurs, et al., 1984). This kind of distribution could be related to relatively abundant prey in these areas, which is supported by

stomach content analyses (Fiedler and Bernard, 1987). Oceanographic cruise data from 1972-1974, combined with concurrent commercial fishery data, show that albacore tend to aggregate on the warm, clear side of upwelling fronts in oceanic waters (Laurs and Lynn, 1991). Recently, the availability of a sufficiently long time series of high-resolution satellite remote sensing data have allowed for the analysis of the relationships between albacore distribution and oceanographic features. For example, Zainuddin et al. (2011) simulated the albacore seasonal migration in the western Pacific Ocean from November 1998 to March 1999, using a kinesis model with sea surface temperature (SST) data derived from the Tropical Rainfall Measuring Mission (TRMM)/TRMM Microwave Imager (TMI), and found that albacore tuna tended to aggregate in the areas near the 20°C isotherm and that they exhibited a latitudinal seasonal migration pattern.

The NEPO contains three major oceanographic water types: subtropical, subarctic, and transition waters (Lynn, 1985). The southern part of the NEPO is dominated by the subtropical gyre consisting of relatively homogeneous oligotrophic waters. There is increasing evidence that this subtropical gyre exhibits substantial physical-biological variability on different time scales (Karl, 1999). The subarctic gyre with its nutrient-rich waters dominates in the northern part of the NEPO, but lots of species are unable to tolerate the cold temperatures in this region. Many species take advantage of the NPTZ between these two basin-scale gyres because of the relatively high food availability at optimal temperature ranges. Despite the semi-permanent large spatial scale of the NPTZ, meso-scale perturbations often dominate in the NPTZ, with many temporally variable fronts forming (Roden, 1991). These fronts are a favored habitat for highly migratory species such as tunas, squids and marine mammals (Bakun, 1996; Polovina et al., 2001).

In this paper, we relate the spatial and temporal distribution of north Pacific albacore CPUE, which is an indicator of albacore distribution, to the location and strength of subtropical fronts in the NEPO over very large temporal (30 years) and spatial scales (entire NEPO). This approach allows us to test the robustness of these relationships on scales pertinent to stock assessments of this stock. In this study, we derived sea surface temperature (SST) gradient grids over the entire NEPO and identified oceanic fronts from SST images using frontal detection algorithms. Frontal parameters were then matched with corresponding albacore surface fishery data from 1982-2011. Associations between albacore CPUE and subtropical fronts were also examined on seasonal and interannual scales.

## DATA AND METHODS

### Fisheries Data

A database of albacore catch (number of fish) and fishing effort (vessel-days) was assembled from the logbook records of US and Canadian albacore troll and pole-and-line vessels, which were extracted from databases maintained by the US National Oceanic and Atmospheric Administration (NOAA)-National Marine Fisheries Service(NMFS) and Department of Fisheries and Oceans Canada. Logbook data from US vessels are available from 1961, but we limited the analysis to data from 1982 to 2011 in order to match the logbook data with remotely-sensed SST data, which are only available from 1982. We limited the analysis of Canadian logbook data to 2004- 2011 because these were considered to be the most reliable data at the time of analysis. The Canadian time series contributed 2.4% to 32.1% of the records in a given year. Subsequently, the data from US and Canadian vessels were assembled into a single database containing fishing date (year, month, day), fishing location (latitude and longitude in degrees and minutes), and total catch (the number of albacore caught plus discarded) for individual vessels. Data from the troll and pole-and-line fisheries were not separated for analysis because logbooks do not record this information and operations of both fisheries are highly similar, with both trolling and pole-and-line fishing operations occurring in the same day. We removed data without location information (latitude and longitude), with locations on land, or located outside of our study area (20-60°N, 110-180°W). After filtering, 289,734 data records remained for analysis. All personal identifying information was removed from the dataset prior to analysis.

### SST, SST gradient and SST front detection

We calculated SST gradients and detected frontal structures using SST grids derived from the Advanced Very High Resolution Radiometer (AVHRR) Pathfinder Version 5.2 (PFV52) daily data with nominal 4 km resolution (ftp://ftp.nodc.noaa.gov/pub/data.nodc/pathfinder/Version5.2/) for our study area, which extended from 19 to 60ºN and from 109 to 180ºW. A total of 10,532 daily images from 1982 to 2011 were downloaded in order to analyze the persistence of fronts in the study area. Smoothed monthly SST values were derived by averaging daily images, and subsequently smoothing with a median filter with 1x1 degree window. The use of monthly averaged SST and spatial smoothing substantially reduces the proportion of cloud cover and attenuates high spatial frequencies, such as micro to meso-scale eddies, which improves our ability to detect the large-scale fronts of

interest in this study (Fig. S1). These smoothed monthly images were then used to compute the SST gradients and SST fronts.

The fronts identified in this study differ in scale from the common definition of subtropical/subarctic fronts. The terms "subtropical front" and "subarctic front" typically refer to "frontal zones", a broad area often characterized by salinity and/or temperature changes (Roden, 1991), and several fronts may occur in each frontal zone. In this study, we are examining the possible association of albacore distribution with individual fronts (i.e., temperature gradients), rather than the much larger frontal zones that may encompass several SST gradients.

Two widely-used frontal detection approaches were applied in this study: the gradient-based method and the histogram method (Belkin and O'Reilly, 2009). Before using these two algorithms, we used the standard approach of applying a Gaussian filter with sigma=1 and window size of 5x5 pixels to the smoothed image. The gradient frontal detection method is relatively simple and is implemented by convolving the SST image with the following function: $G = \sqrt{G_x^2 + G_y^2}$,

where $G_x = P_{i+1,j} - P_{i-1,j}$, $G_y = P_{i,j+1} - P_{i,j-1}$, and P(i,j) are the coordinates of each pixel in the image.

We also used an updated version of the Cayula and Cornillon (1992, 1995) front detection algorithm adapted for upwelling systems (Nieto et al., 2012). By dividing the image into sub-windows, this histogram method evaluates the probability of an edge being present in each sub-window. The SST histograms were analyzed to determine the presence of any bi-modality, indicating the possible presence of two different water masses, and determining the temperature that best separates the two water masses (Fig. S1). We only used the histogram method to mark the presence of a front and used SST gradients to indicate the strength of the front. For example, in August 2000, fronts are widespread throughout the study region, and the stronger fronts with greater SST gradient values are near the NPTZ. The advantage of this front detection approach, compared to the gradient-based method, which generates a continuous field of values, is that only the edges are retained between two water masses, from which the distance from fishing locations to the nearest front can be computed.

Climatological mean conditions

We compared the climatological mean distribution of subtropical fronts in the NEPO with the average albacore spatial distribution in the region. Once the monthly SST gradient grids were calculated as described above, we averaged the SST gradients at each pixel over 30 years (1982 – 2011) to obtain the climatological mean SST

gradient grid. This mean SST gradient grid was further averaged in the latitudinal band (30-45°N) from 180-120°W to obtain the longitudinal differences in mean SST gradient. The latitudinal patterns in mean SST gradient in the NPTZ were determined by averaging the SST gradient in the longitudinal band (180-130°W) from 20-55°N. A bootstrapping method was used to estimate the mean and standard deviation of albacore CPUE with respect to longitude and latitude. The albacore data were subsetted into 1° bins and the numbers of observations in each bin were counted. For each bootstrap run (N=10,000), we resampled the data in each bin with replacement and subsequently calculated the mean CPUE and standard deviation from the bootstrap runs.

Centroid analysis

We applied centroid analysis to study the seasonal and interannual dynamics of SST gradients and their influence on albacore CPUE in the NPTZ. The latitude of the centroids of albacore CPUE in the NPTZ was compared to the latitude of centroids of SST gradients on seasonal and interannual timescales. The domain for NPTZ was delineated as 180-130°W and 30-50°N. We averaged the monthly SST gradient grids and computed the SST gradient centroid in the NPTZ for the fishing season (May to November) over 30 years and did the same for the corresponding albacore CPUE centroid. Mean centroids were the weighted average of SST gradients and CPUE by latitude:

$$mean\ SST\ Grad\ Centroid = \frac{\sum_{i=1}^{n} Latitude_i \cdot SST\ Grad_i}{\sum_{i=1}^{n} SST\ Grad_i}$$

$$mean\ Albacore\ Centroid = \frac{\sum_{i=1}^{n} Latitude_i \cdot CPUE_i}{\sum_{i=1}^{n} CPUE_i}$$

The standard deviations of both centroids were calculated as follows:

$$Standard\ deviation_{SST\ Grad\ Centroid} = \sqrt{\frac{\sum_{i=1}^{n}(Latitude_i - mean\ SST\ Grad\ Centroid)^2 \cdot SST\ Grad_i}{\sum_{i=1}^{n} SST\ Grad_i}}$$

$$Standard\ deviation_{Albacore\ Centroid} = \sqrt{\frac{\sum_{i=1}^{n}(Latitude_i - mean\ Albacore\ Centroid)^2 \cdot CPUE_i}{\sum_{i=1}^{n} CPUE_i}}$$

Both SST gradient and albacore CPUE centroids were calculated for each month and year. The annual centroids were deseasoned by subtracting the mean monthly centroids. The annual mean CPUE centroid of a given year was calculated as the mean deseasoned centroid of all the active fishing months within that year. The annual SST

gradient centroid was the mean deseasoned centroid of the same fishing months. Annual time series of CPUE and SST gradient centroids were normalized [(value – mean)/standard deviation] and a linear regression was performed to study the association of albacore CPUE with SST gradient centroids.

Distance to front and SST gradient strength

After using an updated version of the Cayula and Cornillon method (Nieto et al., 2012) to detect fronts in the NEPO, we calculated the distance from each fishing location to the nearest front. For this portion of the study, we only used fine resolution fisheries data (both degree and minute recorded) because the distances calculated would be less accurate otherwise. In years and months with high cloud coverage the calculated distance from the fishing location to a front may be biased because the nearest front is not observable (Fig. S2). Therefore, we investigated eliminating data records with high cloud cover. A preliminary analysis indicated that the results were not affected by the filter used (size of window and maximum cloud cover percentage), but it was important that a filter was used to eliminate records with high cloud cover (Tab. S1). For this analysis, we decided to remove fisheries data with more than 60% cloud cover within a 5x5 cell window around the fishing location prior to further analysis to minimize this bias, which resulted in the removal of 7.94% of the original data. In addition to distance to the nearest front, we also determined the relationship between albacore CPUE and the SST gradient of the nearest front.

Similar to the abovementioned analysis of albacore CPUE with respect to latitude and longitude, a bootstrapping method was used to estimate the mean and standard deviation of CPUE with respect to distance to front and SST gradient of the nearest front. We first subset the albacore data into 100 km and 0.04°C $km^{-1}$ bins respectively, and counted the number of observations in each bin. For each bootstrap run (N=10,000), we resampled the data in each bin with replacement and subsequently calculated the mean CPUE and the standard deviation from the bootstrap runs. Front detection was performed by Interactive Data Language (IDL) and all other analyses in this study were performed using Matlab R2013a (Mathworks Inc.).

RESULTS

Climatological mean conditions

The longitudinal and latitudinal patterns in albacore CPUE correspond well to the spatial distribution of SST gradients over 30 years. Fig. 2 shows the climatological mean SST gradient of the NEPO from 1982 to 2011. The SST gradients tend to decrease from west to east along the NPTZ, reaching a minimum around 130°W, before rapidly increasing near the coast (Fig. 2). Albacore CPUE generally increases from west to east along the NPTZ but rapidly decreases to a minimum around 132-135°W, which coincides with the SST gradient minimum albeit with a westward bias of approximately 1-4° in longitude (Fig. 3a). Similar to SST gradients, albacore CPUE then rapidly increases to a maximum that is approximately 2-3° west of the maximum SST gradient near the coast. The latitudinal patterns in albacore CPUE also correspond well to the latitudinal changes in SST gradients. The climatological mean SST gradients peak at approximately 40°N and the albacore CPUE follows a similar pattern, increasing to a peak around 40 to 45°W (Fig. 3b).

Seasonal variation

Seasonal variation of the albacore CPUE centroid corresponded well to seasonal changes in the SST gradient centroid in the NPTZ (Fig. 4). The seasonal movements of both centroids, moving north in summer and south in fall, are strongly correlated ($R^2$=0.908, $p<0.001$). However, the albacore CPUE centroid showed a substantially larger variation in position than the SST gradient centroid. The mean albacore centroid had a seasonal variation of almost 10° of latitude, whereas the mean SST gradient centroid had a variation of about 1 to 2° of latitude. The standard error of SST gradient centroid and albacore centroid were ±6° and ±2°, respectively.

Interannual variation

Interannual changes in the albacore CPUE centroid generally corresponded well to the interannual variability exhibited by the SST gradient centroid (Fig. 5a, $R^2$ = 0.43) with the exception of several years from the late 1980s to early 1990s and after 2003. The numbers of observations in the NPTZ in 1988-1990 and after 2003 were relatively small (N < 1,000 vessel days) (Fig. 5b) compared to the rest of the time series. During these periods, the open ocean was poorly sampled relative to the coastal areas due to changes in fishery operations (Tab. S2). Details on these changes in fishery operations can be found in other places (Teo et al., 2010; Xu et al., 2013). As a result, the calculated albacore centroid in the open ocean is likely subject to greater uncertainty due to small sample sizes in those years. The same analysis was conducted on data from US vessels only (i.e., with Canadian vessels

removed) and similar results were obtained. The normalized albacore centroid time series exhibited a significant linear relationship with the normalized SST gradient centroid (Fig. 6) ($R^2$ = 0.33; p=0.0017).

Front analyses and Sensitivity studies

Average albacore CPUE tended to decrease with increasing distance from the nearest front while exhibiting a dome-shaped relationship with the strength of SST gradients of the nearest front (Fig. 7). Overall, the albacore tended to aggregate near the front, with the highest CPUE occurring within 100 km of the front. Albacore CPUE showed a substantial reduction from the front to 500km (Fig. 7a). A significant negative relationship was found between mean CPUE and the distance to the nearest front ($p < 0.001$, $R^2$=0.949). On the other hand, albacore CPUE exhibited a dome-shaped response to the SST gradient of the nearest front, reaching a maximum when SST gradient was 0.12-0.16°C $km^{-1}$ (Fig. 7b).

DISCUSSION

Like other tuna and highly migratory species, albacore has long been known to be associated with oceanic fronts, with fishermen often fishing along these fronts (Shomura and Otsu, 1956; Graham, 1957; McGary et al., 1961; Laurs and Lynn, 1977, 1991; Polovina et al., 2001). However, previous work concentrated on the association of albacore with oceanic fronts on relatively fine spatial and temporal scales. In this study, we concentrate on the large-scale patterns by testing the association of albacore with oceanic fronts over the entire NEPO for over 30 years.

On average, areas of high albacore CPUE correspond well to large-scale patterns in SST gradient over the past 30 years. Interestingly, the minimum in albacore CPUE around 132-135°W matches the minimum in SST gradient, albeit with a westward displacement of 1-4° in longitude. This slight westward displacement continues as albacore CPUE and SST gradients rapidly increases near the coast. This displacement between SST gradient and albacore CPUE may be due to strong upwelling and offshore transport near the coast. As the ecosystem develops from upwelled nutrients to phytoplankton, and subsequently to zooplankton and the prey of albacore, strong offshore advection may shift these ecosystem components several hundreds of kilometers offshore (Botsford et al., 2003; Checkley and Barth, 2009). Changes of SST gradient alone do not explain all the variability in albacore abundance

or distribution but this easily-derived variable can be included in statistical models for standardization of CPUE (e.g., Generalized Additive Models) as one of the explanatory variables.

Large-scale spatial differences in albacore CPUE also suggest that the catchability of albacore is likely to be poor in areas with weak SST gradients (e.g., around 132-135°W), even though albacore clearly have to transit this area in order to get nearer to the North American coast. Therefore, when a standardization model for an abundance index based on this fishery is designed, it is important for stock assessment scientists to take account of large-scale changes in SST gradients. Anecdotally, albacore fishermen in this fishery have suggested that they can observe tuna (likely albacore) on their sonar in the region with low albacore CPUE but the albacore tend not to bite. The results of electronic tagging studies also support the suggestion that albacore spend more time at depth when the mixed layer depth deepens (Childers et al., 2011). Phillips (2011) also found that the scalar wind speed cubed (a proxy variable for mixed layer depth) is associated with albacore CPUE. It would be interesting to examine the depth data from electronically tagged albacore to see if there are behavioral changes when swimming through areas with weak SST gradients. For trans-Pacific species like albacore, it would also be interesting to compare these results in the NEPO with albacore in the western Pacific.

Juvenile albacore migrate in the summer and fall months to the North American coast (Clemens, 1961; Pearcy, 1973; Childers et al., 2011) and back to the NPTZ in winter (Laurs and Nishimoto, 1979; Polovina et al., 2001; Childers et al., 2011). However, based on the logbook data that, there are vessels fishing in the NPTZ with high CPUE during the summer and fall months, thus indicating that even at the peak of the coastal fishing season, some portion of the albacore remained offshore in the NPTZ. This hypothesis is consistent with changes in the seasonal SST gradient. High SST gradient occurs both in the NPTZ and the coast during summer but only in the NPTZ in winter (Fig. S3).

It is interesting to note that no apparent single-year anomaly were found over 30 years (Fig. 5), therefore we speculate that there were no substantial differences in the albacore CPUE spatial patterns in the NPTZ during El Niño events. The strongest El Niño events over the past 30 years occurred in 1982-83 and 1997-98 but both albacore and SST gradient centroids in those years appeared to be similar to non-El Niño years. A closer visual inspection of the SST gradient or frontal occurrence maps during those El Niño years also did not reveal substantial differences during those years.

There are interannual changes in the 'hotspot' areas with high albacore CPUE along the NPTZ (Fig. S4) but the environmental predictors for these hotspots in the NEPO remain relatively unclear. Previous studies in the NEPO have identified environmental variables including water temperature, food availability, and SST and chlorophyll fronts as being important drivers (Johnson, 1962; Laurs and Lynn, 1977, 1991; Polovina et al., 2001) but these studies did not investigate the effect of interannual variability of these environmental variables over the long term. Recently, Phillips et al.(2014) published a study on the spatio-temporal associations of albacore CPUEs with environmental variables along the North American coast (east of 130°W), but unfortunately did not include the NPTZ within their study area.

The centroid analyses successfully explained the interannual variability of latitudinal changes in albacore distribution but interannual changes in longitudinal albacore distribution do not appear to be related to either SST gradient or oceanic front structure (Fig. S4). These longitudinal changes could be related to other biological (migration pattern, prey distribution, behavior changes) or physical factors (e.g., currents, horizontal or vertical transport) (Chelton, et al., 1982). Electronic tagging datasets (Childers et al., 2011) may be a useful resource for testing these hypotheses for north Pacific albacore in the NEPO or other regions of the Pacific Ocean or other highly migratory species.

Previous studies in other oceanic regions have examined the environmental influences on hotspots of albacore CPUE. Hot spots for albacore in the northwestern Pacific from 1998 to 2003 appeared to occur in areas with warmer SST (19.78°C), relatively high chlorophyll concentrations (0.31 $mg \cdot m^{-3}$), and high eddy kinetic energy and geostrophic currents (Zainuddin et al., 2006, 2008). In the Northeast Atlantic, an analysis with generalized additive models found that SSTs of 16-18°C are preferred but there were also high CPUE areas that did not appear to be related to thermal gradients (Sagarminaga and Arrizabalaga, 2010). Lan et al. (2012) related albacore distribution to SST and Jensen-Shannon divergence (an index of SST gradient-like or relative SST gradient, ranging from 0 to 1) in the Indian Ocean from 2006 to 2008 and found that high CPUE occurred at SSTs of 15-19°C and moderate to high Jensen-Shannon divergence values (0.3-0.9). In contrast to these analyses, we considered both the gradient-based (strength of the front) and histogram-based thermal structure (presence and edge of the front) simultaneously, and it would be interesting to apply the current method to other regions and examine whether results are consistent.

Laurs and Lynn (1977) proposed three hypotheses for the association of albacore with thermal fronts: habitat temperature preference, biological productivity and thermal gradient as they affect thermoregulation processes. Neill (1976) suggested that it is energy efficient for fishes to aggregate near narrow thermal discontinuities (fronts). The habitat preference hypothesis helps us define a broad range of optimal temperature zones (16-19°C, primarily in NPTZ and North American coast) and eliminate the Alaska region (which also has high SST gradients) as an area of albacore preferred habitat. High thermal gradient areas are often related to nutrient-rich waters with high productivity. Both tagging and stomach content data support hypothesis that albacore consume a variety of prey species in the NPTZ and the North American coast (Pinkas et al., 1971), although the average volumes consumed were comparable in both areas (Laurs and Lynn, 1977, 1991). Polovina et al. (2001) studied albacore associated with the chlorophyll front in the NPTZ and suggested that 0.2 mg $m^{-3}$ may be the northern limit for albacore distribution. However, the distribution of zooplankton or planktivorous fish in the NPTZ is an important link between the ocean physics and a top predator like albacore and should be evaluated.

The findings of this study will likely help improve the development of abundance indices based on US and Canadian surface fishery data used in the albacore stock assessment by incorporating environmental indices (SST gradients or frontal probability) into the standardization process. The 2011 stock assessment (ISC, 2011) did not explicitly accounted for changes in catchability or availability related to variation in the spatial distribution and catchability of albacore in the NEPO in response to environmental variability. Instead, the assessment assumed a larger coefficient of variation (CV) for this index due to this uncertainty. In the most recent assessment (ISC, 2014) environmental information was used to identify specific subareas with potential differences in catchability, which were then incorporated into the standardization model. For example, a large drop in CPUE in the region between the NPTZ and coastal areas appear to be related to a corresponding drop in SST gradient. This subarea was included in the standardization model to help explain potential changes in catchability in different areas, which likely improved the resulting albacore abundance index (Xu et al. 2014).

ACKNOWLEDGEMENTS

This research was supported by NOAA-FATE program. The authors acknowledge all US and Canadian fishermen who reported the albacore catch data in logbooks. The satellite data were provided by GHRSST and the US National Oceanographic Data Center, partially supported by the NOAA Climate Data Record (CDR) Program. We thank three internal reviewers (Dr. Paul Fiedler, Dr. Christian Reiss and Dr. Tim Sippel) and three anonymous reviewers for their useful comments and suggestions.

REFERENCES

Bakun, A., 1996. Patterns in the ocean. La Paz, Mexico. California Sea Grant College/ CIB, p. 323.

Belkin, I.M., and O'Reilly, J.E., 2009. An algorithm for oceanic front detection in chlorophyll and SST satellite imagery. Journal of Marine Systems 78 (3), 317-326.

Botsford, L.W., Lawrence, C.A., Dever, E.P., Hastings, A., Lagier, J., 2003. Wind strength and biological productivity in upwelling systems: an idealized study. Fisheries Oceanography 12, 245-259.

Cayula J.F., and Cornillon, P., 1992. Edge detection algorithm for SST images. Journal of Atmospheric and Oceanic Technology 9, 67-80.

Cayula J.F., and Cornillon, P., 1995. Multi-image edge detection for SST images. Journal of Atmospheric and Oceanic Technology, 12, 821-829.

Checkley, D.M., and Barth, J.A., 2009. Patterns and processes in the California Current System. Progress in Oceanography 83, 49-64.

Chelton, D., Bernal, P., and McGowan, J. 1982. Large-scale interannual physical and biological interaction in the California Current. Journal of Marine Research 40, 1095–1125.

Childers, J., Snyder, S., and Kohin, S., 2011. Migration and behavior of juvenile North Pacific albacore (*Thunnus alalunga*). Fisheries Oceanography 20(3), 157-173.

Clemens, H.B. 1961. The migration, age, and growth of Pacific albacore (*Thunnus germo*), 1951-1958. Fish Bulletin 115, 128pp.

Fiedler, P.C., and Bernard, H.J., 1987. Tuna aggregation and feeding near fronts observed in satellite imagery. Continental Shelf Research 7, 871-881.

Graham, J.J., 1957. Central North Pacific albacore surveys, May to November 1955. U.S. Fish Wildlife Service, Special Scientific Report Fisheries 212, p.38.

Ichinokawa, M., Coan, A.L. Jr., and Takeuchi, Y., 2008. Transoceanic migration rates of young North Pacific albacore, *Thunnus alalunga*, from conventional tagging data. Canadian Journal of Fisheries and Aquatic Sciences 65, 1681-1691.

ISC, 2011. Report of 11th meeting the albacore working group workshop. 20-25 July 2011, San Francisco, California, USA. Stock assessment of albacore tuna in the North Pacific Ocean in 2011.

ISC, 2014. Report of the albacore working group workshop. 16-21 July 2014, Taipei, Taiwan. Stock assessment of albacore tuna in the North Pacific Ocean in 2014. Available at: http://isc.ac.affrc.go.jp/pdf/ISC14pdf/ISC14_Plenary_Report_draft%20cleared%20140721-2_2Sept14_sms_forpostingonweb.pdf

Johnson, J.H. 1962. Sea temperatures and the availability of albacore off the coasts of Oregon and Washington. Transactions of the American Fisheries Society 91(3), 269-274.

Karl, D., 1999. A sea of change: biogeochemical variability in the North Pacific Subtropical Gyre. Ecosystems 2, 181-214.

Lan, K.W., Kawamura, H., Lee, M.A., Lu, H.J., Shimada, T., Hosoda, K., Sakaida, F., 2012. Relationship between albacore (*Thunnus alalunga*) fishing grounds in the Indian Ocean and the thermal environment revealed by cloud-free microwave sea surface temperature. Fisheries Research 113, 1–7.

Laurs, R.M. and Lynn, R.J., 1991. North Pacific albacore ecology and oceanography. In J.A. Wetherall (Ed.), Biology, oceanography and fisheries and the North Pacific Transition Zone and Subarctic Frontal Zone. NOAA Technical Report NMFS 105, p. 69-87.

Laurs, R.M., and Lynn, R.J., 1977. Seasonal migration of North Pacific albacore, *Thunnus alalunga*, into North American coastal waters: distribution, relative abundance, and association with transition zone waters. Fisheries Bulletin U.S. 75, 795.

Laurs, R.M., and Nishimoto, R., 1979. Summary of findings made by vessels on charter to the Pacific Tuna Development Foundation. NMFS Southwest Fisheries Sciences Center Administration Report 111-79-5, p. 38.

Laurs, R.M., Fiedler, P.C., and Montgomery, D.R., 1984. Albacore tuna catch distributions relative to environmental features observed from satellites. Deep-Sea Research 31, 1085-1099.

Lynn, R.J., 1985. The subarctic and Northern Subtropical Fronts, in the Eastern North Pacific Ocean in Spring. Journal of Physical Oceanography 16(2), 209-222.

McGary, J.W., Graham, J.J., and Otsu, T., 1961. Oceanography and North Pacific albacore. California Cooperative Oceanic Fisheries Investigations Report 8, 45-53.

Neill, W.H., 1976. Mechanisms of behavioral thermoregulation in fishes. Report of Workshop on the Impact of Thermal Power Plant Cooling Systems on Aquatic Environments. Electric Power Research Institute Special Report 38, 156-169.

Nieto, K., Demarcq, H., and McClatchie, S., 2012. Mesoscale frontal structures in the Canary Upwelling System: new front and filament detection algorithms applied to spatial and temporal patterns. Remote Sensing of Environment 123, 339–346.

Otsu, T., and Uchida, R.N., 1963. Model of the migration of albacore in the North Pacific Ocean. Fishery Bulletin U.S. 63, 33-44.

Pearcy, W.G, 1973. Albacore oceanography off Oregon-1970. Fishery Bulletin U.S. 71, 489-504.

Phillips, A.J., 2011. Long term albacore (*Thunnus alalunga*) spatio-temporal association with environmental variability in the Northeastern Pacific. MS Thesis. Oregon State University.

Phillips, A.J., Ciannelli, L., Brodeur, R.D., Pearcy, W.G., and Childers, J., 2014. Spatio-temporal associations of albacore CPUEs in the Northeastern Pacific with regional SST and climate environmental variables. ICES Journal of Marine Science, doi.10.1093/icesjms/fst238.

Pinkas, L., Oliphant, M.S., Iverson, I.L.K., 1971. Food habits of albacore, Bluefin tuna, and bonito in California waters. California Department of Fish and Game, Fish Bulletin 152, p.105.

Polovina, J.J., Howell, E., Kobayashi, D.R., and Seki, M.P., 2001. The transition zone chlorophyll front, a dynamic global feature defining migration and forage habitat for marine resources. Progress in oceanography 49, 469-483.

Roden, G.I., 1991. Subarctic-Subtropical Transition Zone of the North Pacific large-scale aspects and mesoscale structure. In J.A. Wetherall (Ed.), Biology, oceanography and fisheries and the North Pacific Transition Zone and Subarctic Frontal Zone. NOAA Technical Report NMFS 105, p. 1-38.

Sagarminaga Y., and Arrizabalaga, H., 2010. Spatio-temporal distribution of albacore (*Thunnus alalunga)* catches in the northeastern Atlantic: relationship with the thermal environment. Fisheries Oceanography 19, 121–134.

Shomura, R.S. and Otsu., T., 1956. Central North Pacific albacore surveys, January 1954-February 1955. U.S. Fish Wildlife Service, Special Scientific Report Fisheries 173, p.29.

Teo, S.L.H., Lee, H.-H., and Kohin, S., 2010. Spatiotemporal characterization and critical time series of the US albacore troll fishery in the North Pacific. Working Paper submitted to the ISC Albacore Working Group Meeting, 20-27 April 2010, Shimizu, Japan. ISC/10-1/ALBWG/05.

Xu Y., Teo, S.L.H., and Holmes, J., 2013. An update of the standardized abundance index of US and Canada albacore troll fisheries in the North Pacific (1966-2012). Working Paper submitted to the ISC Albacore Working Group Meeting, 5-12 November 2013, Shimizu, Japan. ISC/13/ALBWG-03/06. Available at: http://isc.ac.affrc.go.jp/pdf/ALB/ISC13_ALB_2/ISC_13_ALBWG_03_06_Xu_v3.pdf

Xu, Y., Teo, S.L.H., and Holmes, J., 2014. An update of the standardized abundance index of US and Canada Pacific albacore troll and pole-and-line fisheries on the West Coast of North America (1966-2011). Working Paper submitted to the ISC Albacore Working Group Meeting, 14-28 April 2014, La Jolla, USA. ISC/14/ALBWG/03: 8p. Available at: http://isc.ac.affrc.go.jp/pdf/ALB/ISC14_ALB/ISC-14-ALBWG-03-USCA_CPUE_INDEX_Yi_etal-finalversion.pdf

Zainuddin, M., Kiyofugi, H., Saitoh, K., and Saitoh, S., 2006. Using multi-sensor satellite remote sensing and catch data to detect ocean hot spots for albacore (*Thunnus alalunga*) in the northwestern North Pacific. Deep-Sea Research II 53, 419-431.

Zainuddin, M., Saitoh, K. and Saitoh, S., 2008. Albacore (*Thunnus alalunga*) fishing ground in relation to oceanographic conditions in the western North Pacific Ocean using remotely sensed satellite data. Fisheries Oceanography 17, 61-73.

Zainuddin, M., Saitoh, K., and Saitoh, S., 2011. Application of satellite microwave remote sensing data to simulate migration patterns of albacore tuna. ." International Journal of Remote Sensing and Earth Sciences 8, 49-56.

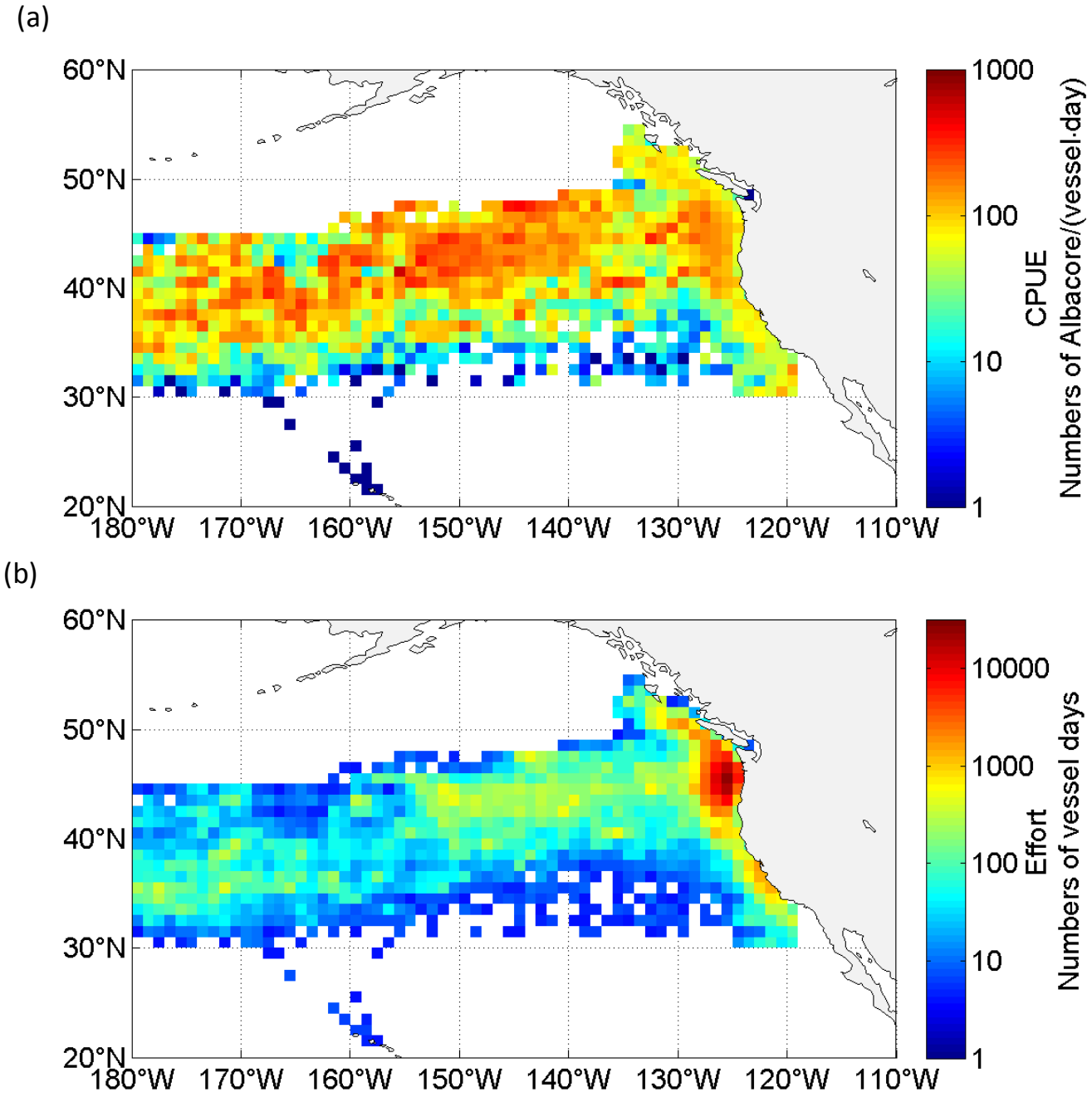


Figure 1. Distribution of US and Canadian troll and pole-and-line fishery (a) CPUE and (b) effort for juvenile albacore in the Northeast Pacific Ocean from 1982-2011. Effort was in unit of numbers of vessel days. CPUE was in unit of numbers of albacore per vessel per day. Both effort and CPUE are plotted in log scale. Strata with <=3 vessels were not shown due to data confidentiality requirements.

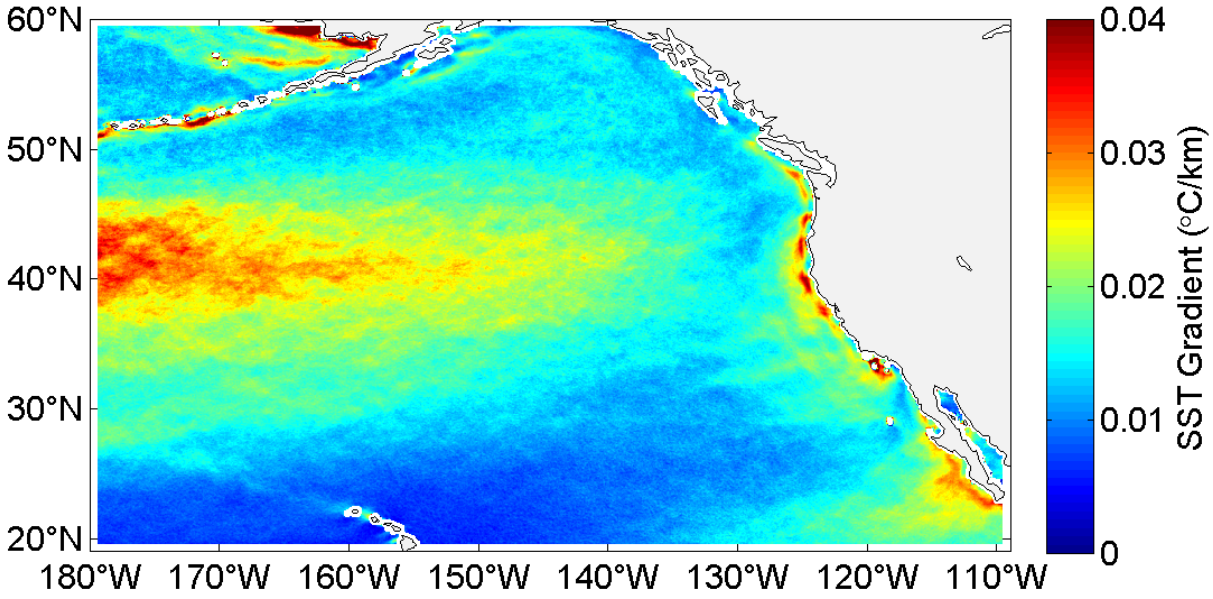


Figure 2. Climatological mean SST gradient in the Northeast Pacific averaged from 1982 to 2011.

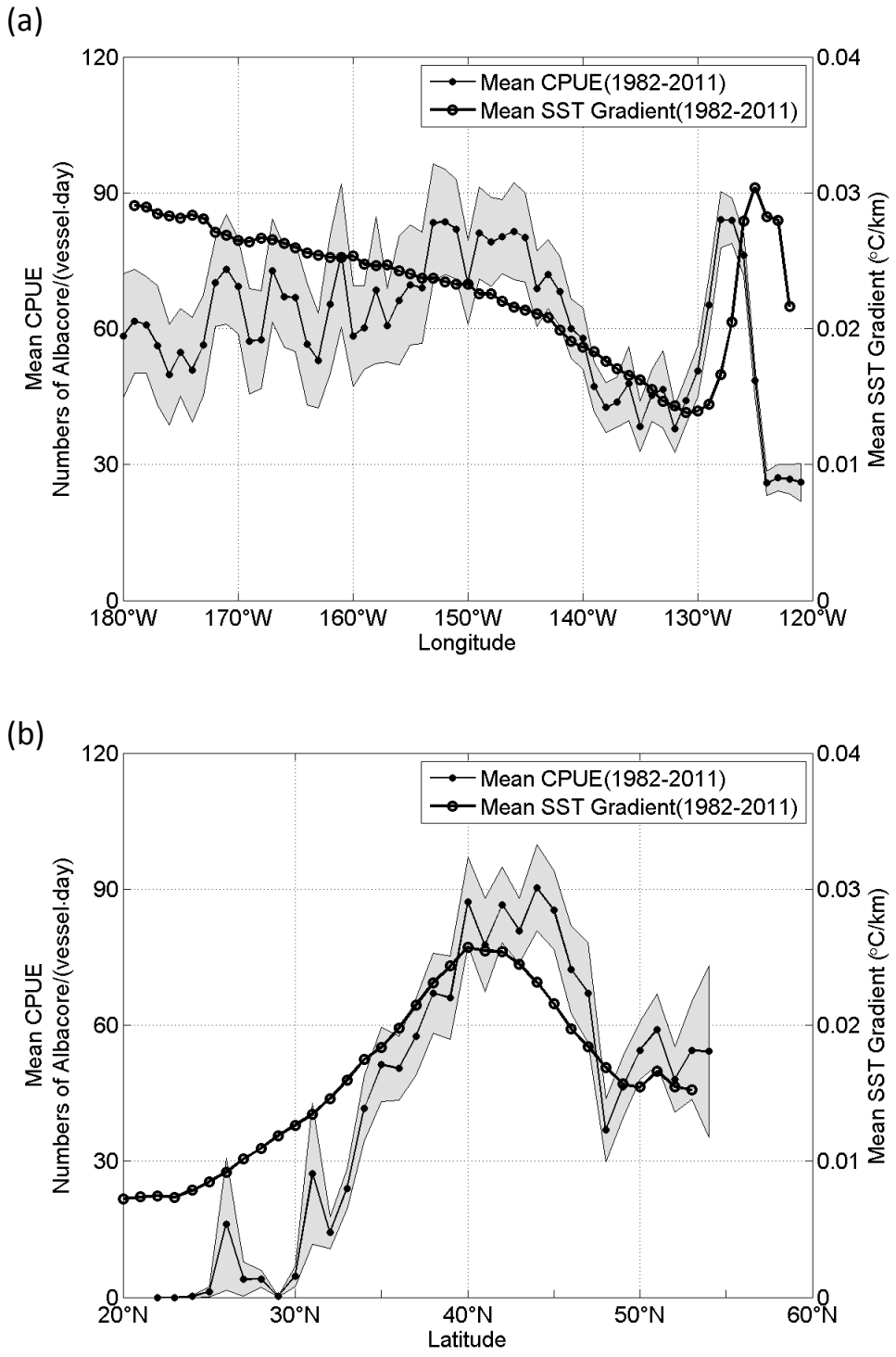


Figure 3. (a) Climatological mean longitudinal distribution of the SST gradient and albacore CPUE during 1982-2011. Mean SST gradient (thick black line) was averaged from 30 to 45°N. (b) Climatological mean latitudinal distribution of the SST gradient and albacore CPUE during 1982-2011. Mean SST gradient (thick black line) was averaged from 180 to 130°W. CPUE was calculated by bootstrapping the logbook data 10,000 times. The thin black line and grey area were the bootstrapped mean and standard deviation of the albacore CPUE, respectively.

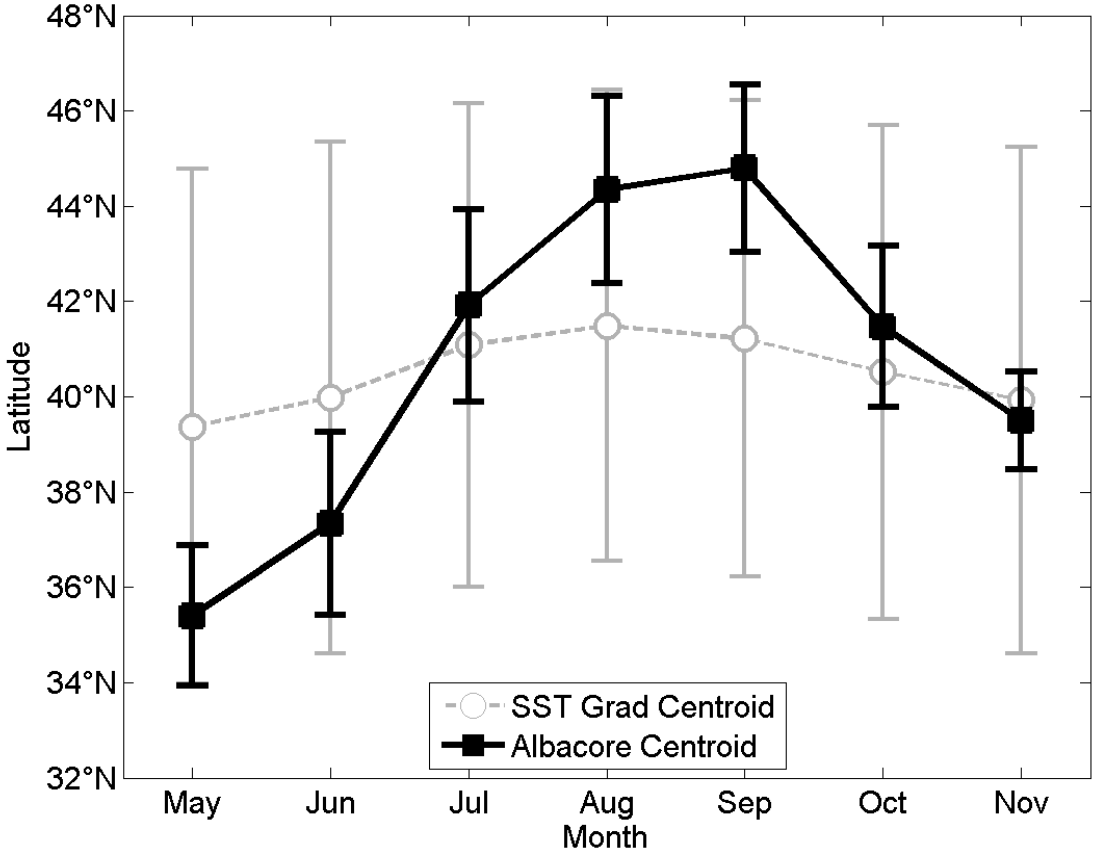


Figure 4. Seasonal variation of mean albacore CPUE centroids (black squares) and mean SST gradient centroids (grey circles) during the fishing season (May-November) from 1982 to 2011. Error bars are one standard deviation from the mean. For each month, the albacore centroid and SST gradient centroid were averaged over the area 30 to 50°N and 180 to 130°W.

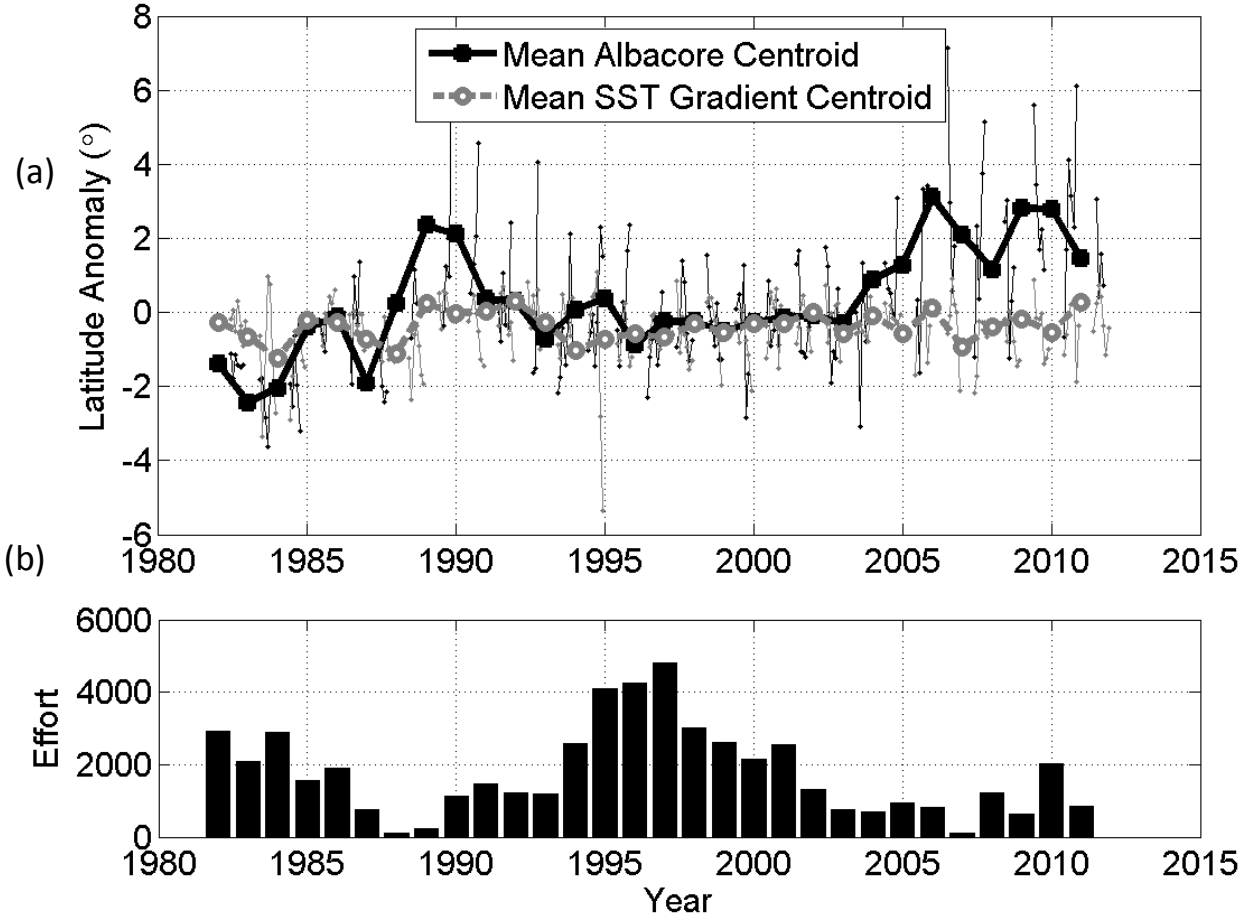


Figure 5. (a) Interannual variation of albacore CPUE centroids and SST gradient centroids during the fishing season (May-November) from 1982 to 2011. For each month, the albacore centroid (black dots) and SST gradient centroid (grey dots) were averaged over the area 30 to 50°N and 180 to 130°W. Annual mean albacore centroids (black squares) were averaged over all fishing months of each year and annual mean SST gradient centroids (grey circles) were averaged over the same fishing months. 6 (b) Annual total fishing effort of albacore during 1982-2011 (units in numbers of vessel days).

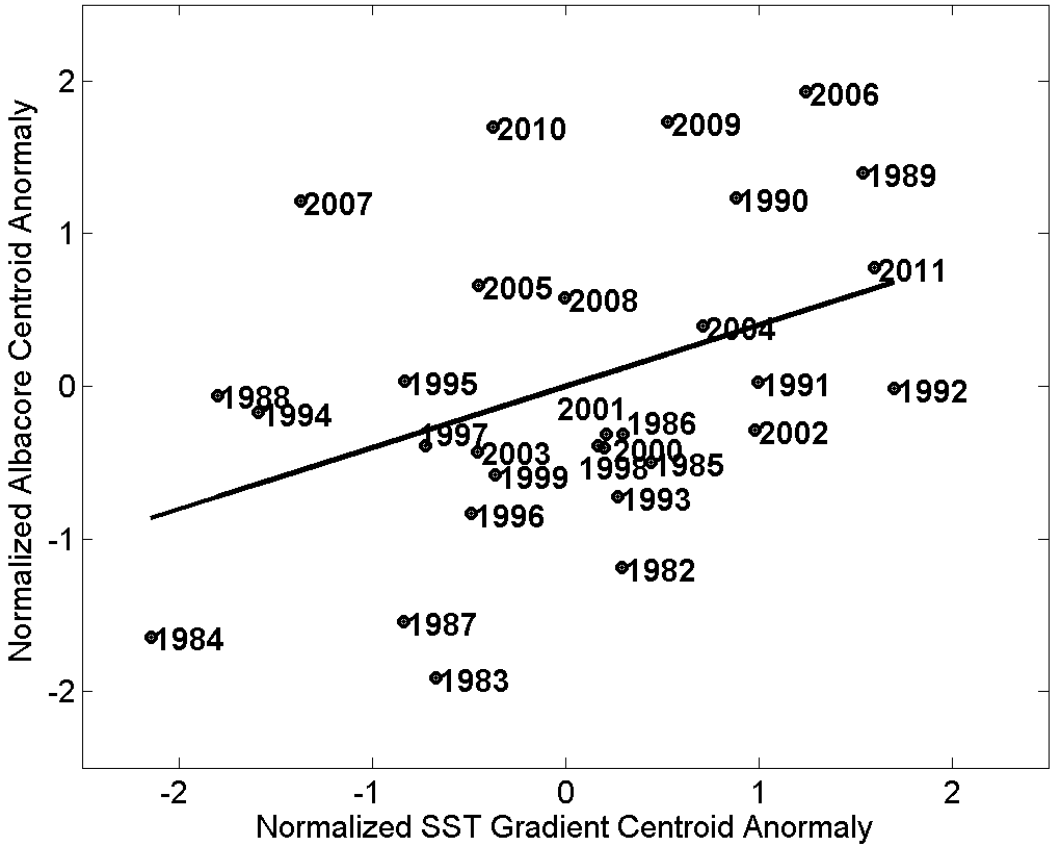


Figure 6. Linear regression between normalized annual mean SST gradient centroid and normalized annual mean albacore CPUE centroid from 1982 to 2011(Albacore centroid=-2.097x$10^{-16}$+0.4022xSST gradient centroid, p-Value<0.05).

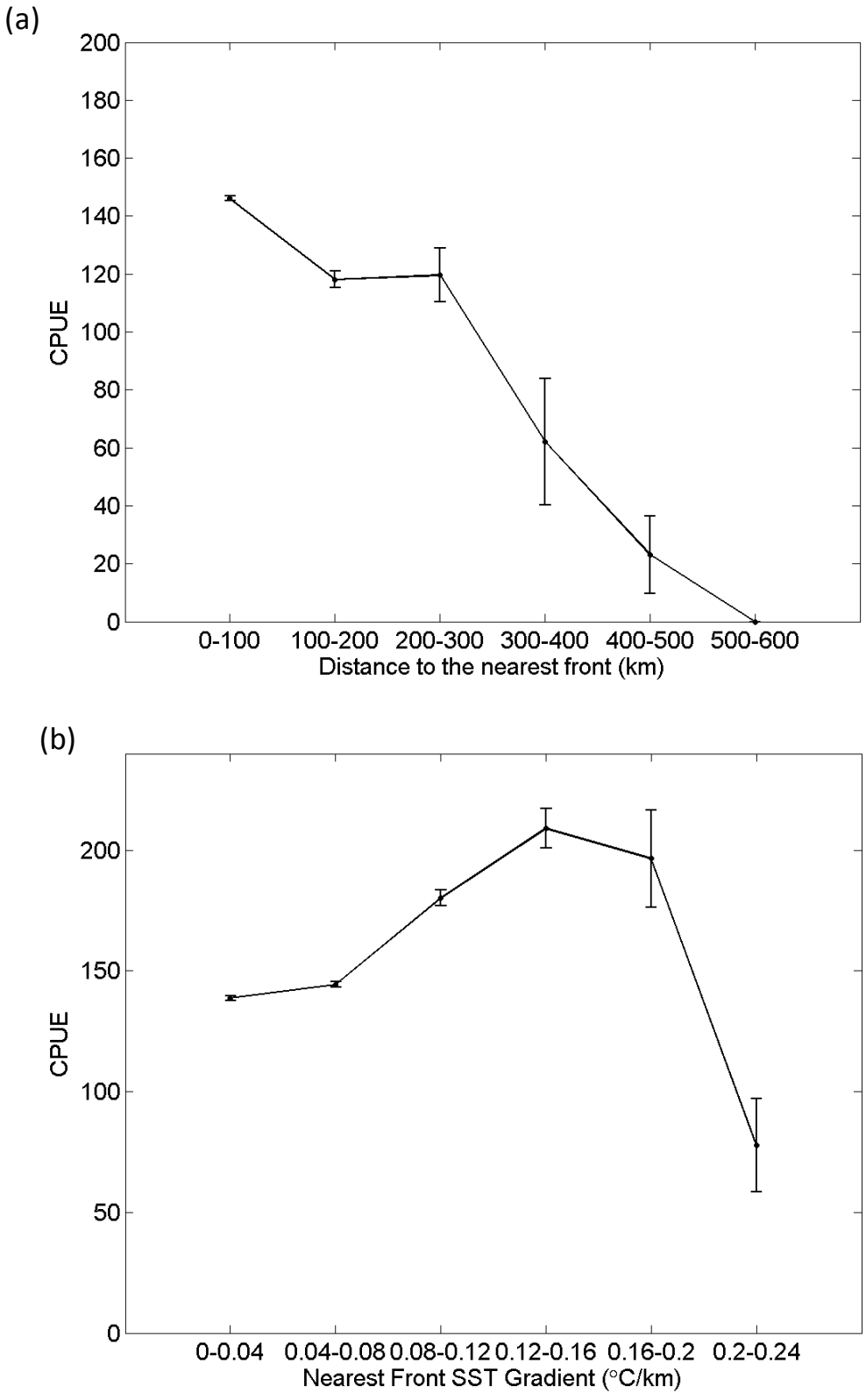


Figure 7. Mean CPUE (fish/vessel-day) with regard to (a) the distance to the nearest front. (b) the nearest front SST gradient. Error bars indicate the standard errors of the 10,000 bootstrapping runs.

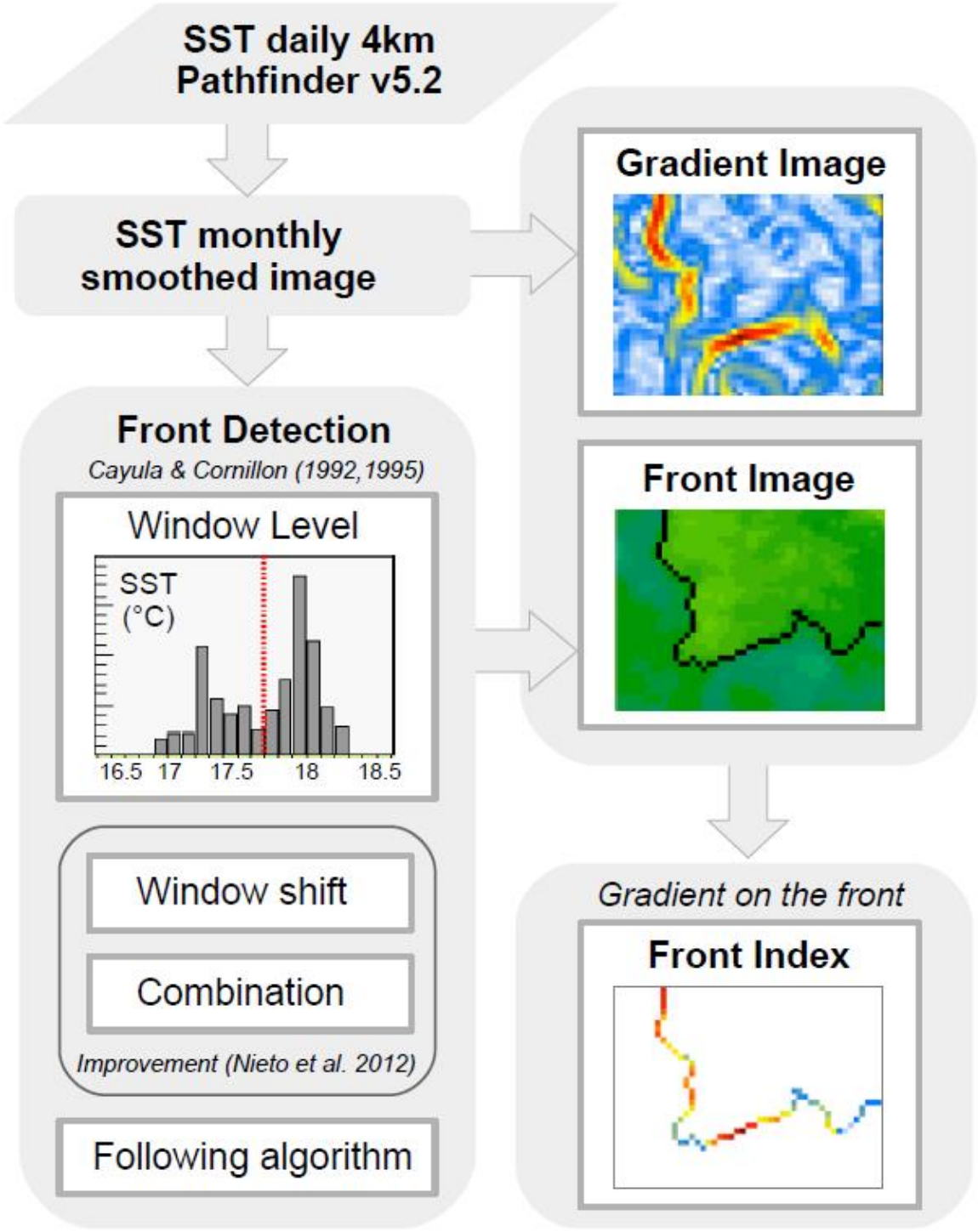


Figure S1. A schematic diagram for the calculation of SST gradients and front detection.

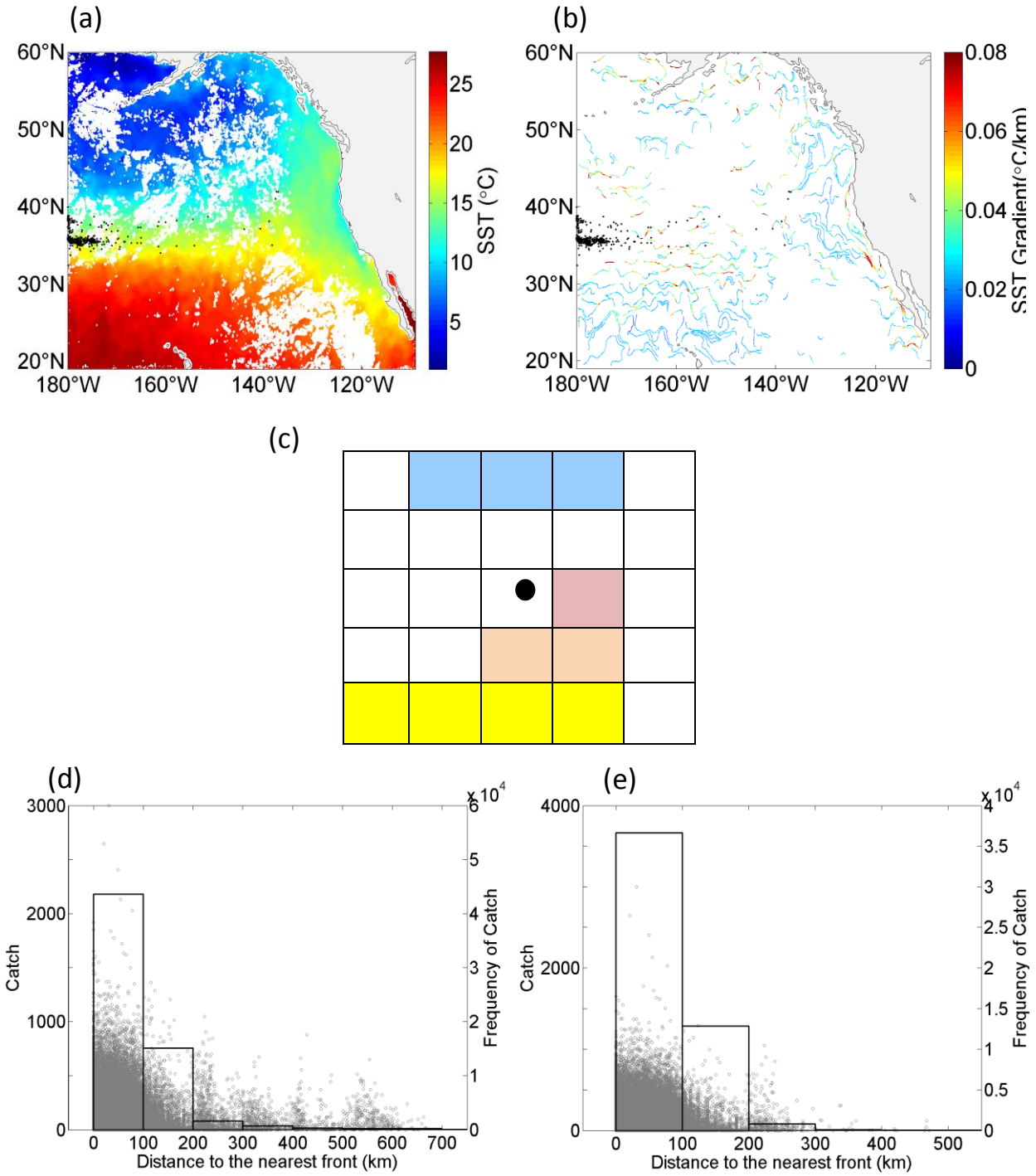


Figure S2. An example of how cloud coverage can affect calculation of distance to front. (a) A SST map with fishing locations (black dots). (b) A front map during the same month. (c) A zoomed illustration of fishing location (black dots), cloud (white grids) and SST (color grids). Front is not detected in this region because of cloud coverage. By applying a filter of 60% (5x5x60%=15 grids), this point is not used in the distance to front calculation. (d) The numbers of catch and catch frequency with regarding to distance to the nearest fronts before applying the filter. (e) The numbers of catch and catch frequency with regarding to distance to the nearest fronts after applying the filter. Note that high catch far from the front were removed after applying a filter.

(a)

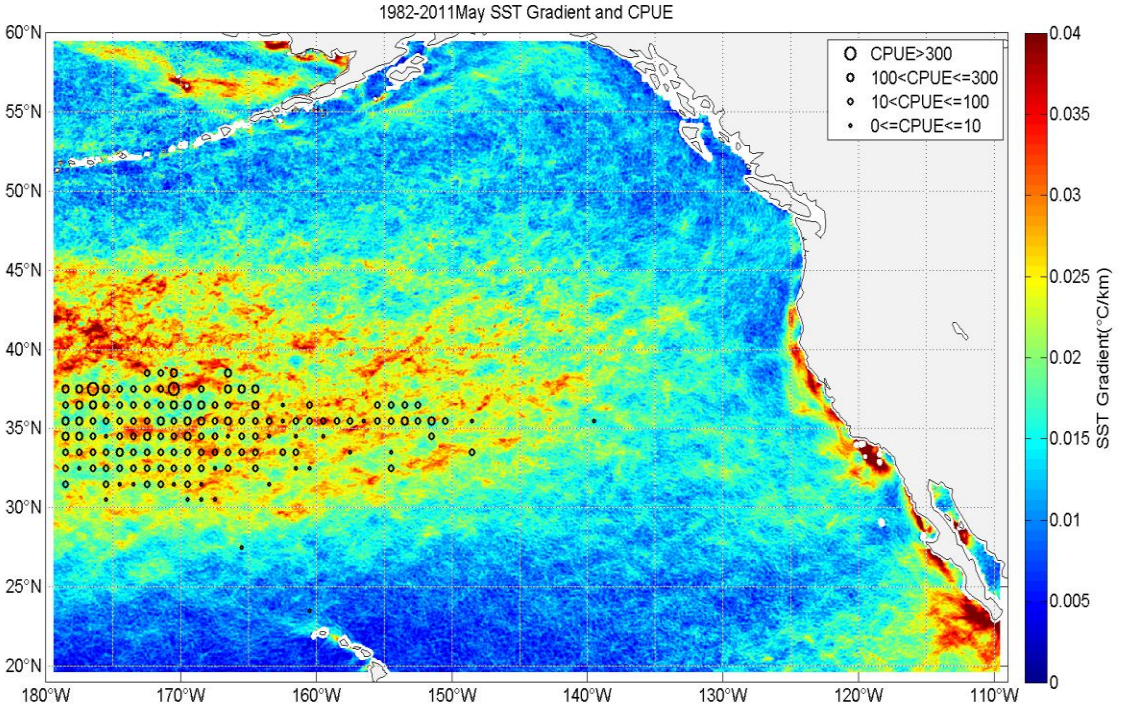


(b)

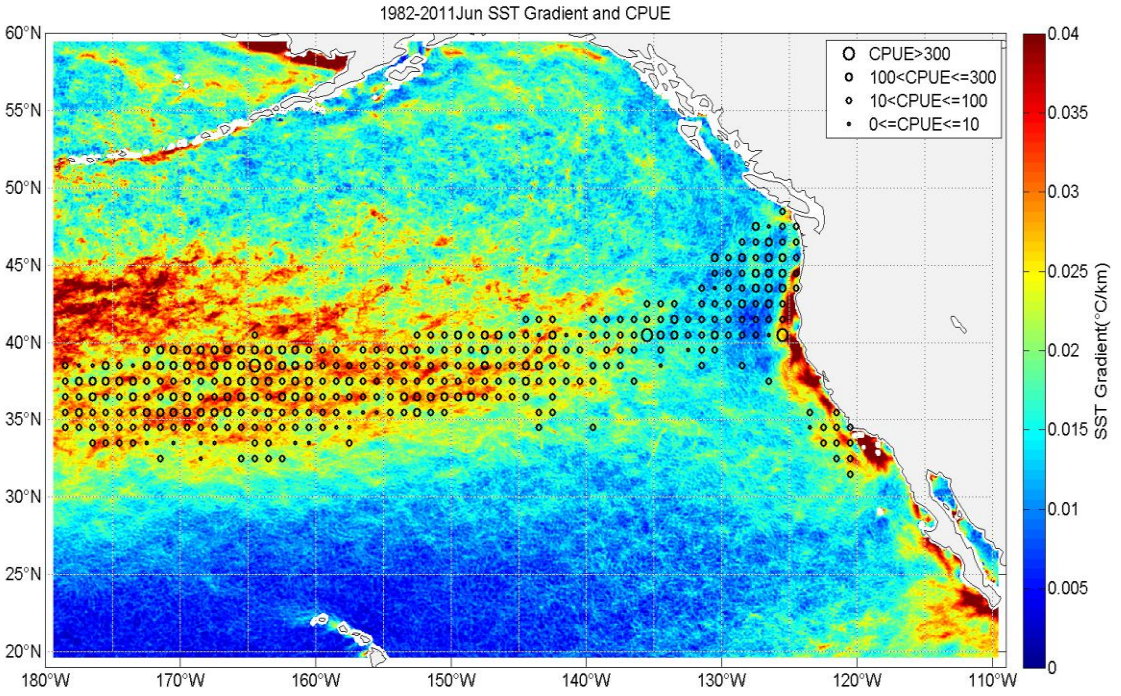


Figure S3. Averaged SST gradient in May (a), June (b), July (c), August (d), September (e), October (f), and November (g) and averaged monthly CPUE (numbers of albacore per vessel per day) in the Northeast Pacific averaged from 1982 to 2011. CPUE is averaged in monthly 1x1 degree strata and is represented on the plot by circles located at the center of each spatial stratum, which may be displayed as being on land.

(c)

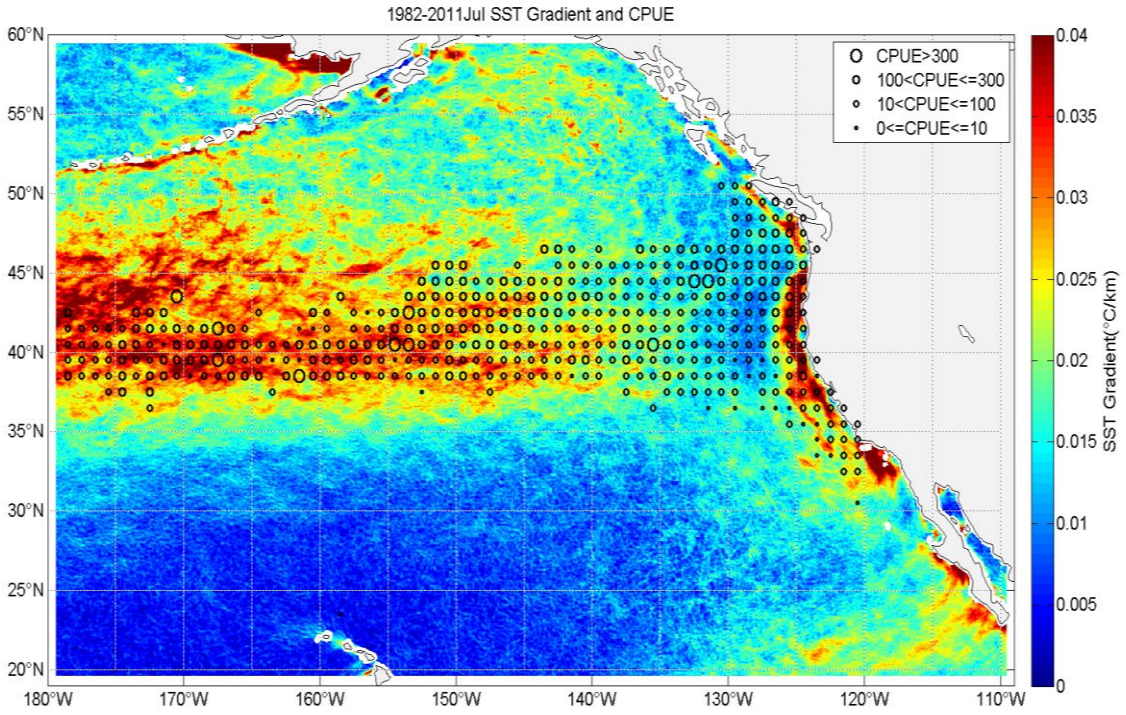


(d)

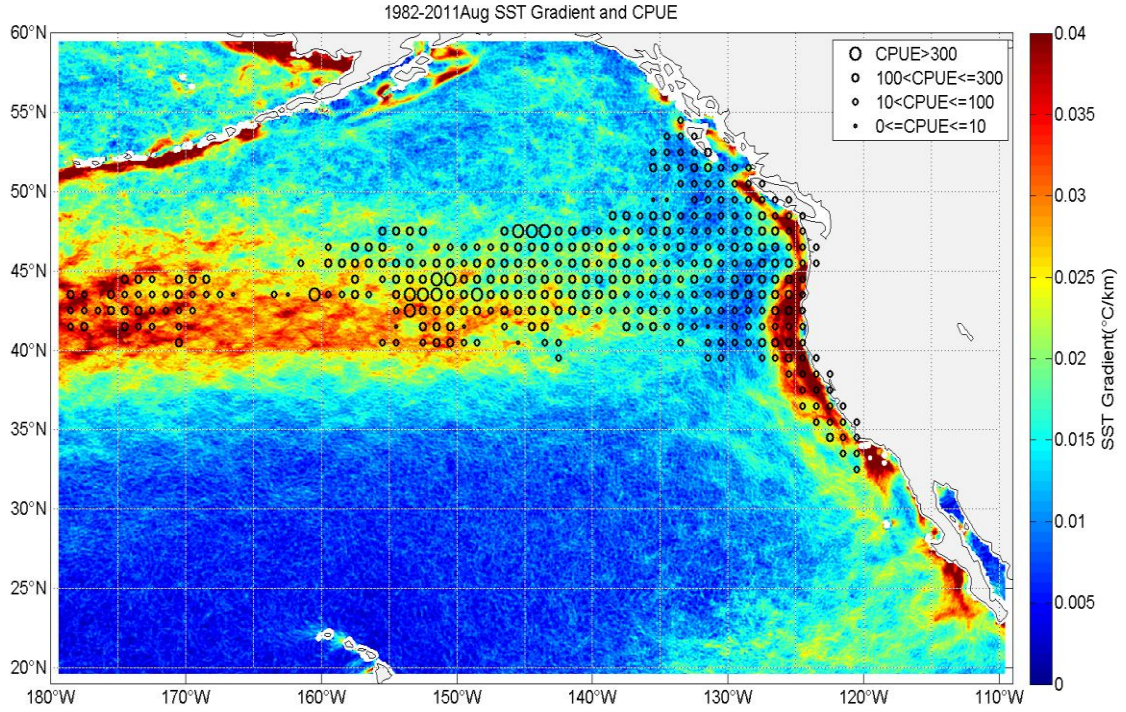


Figure S3. Continued.

(e)

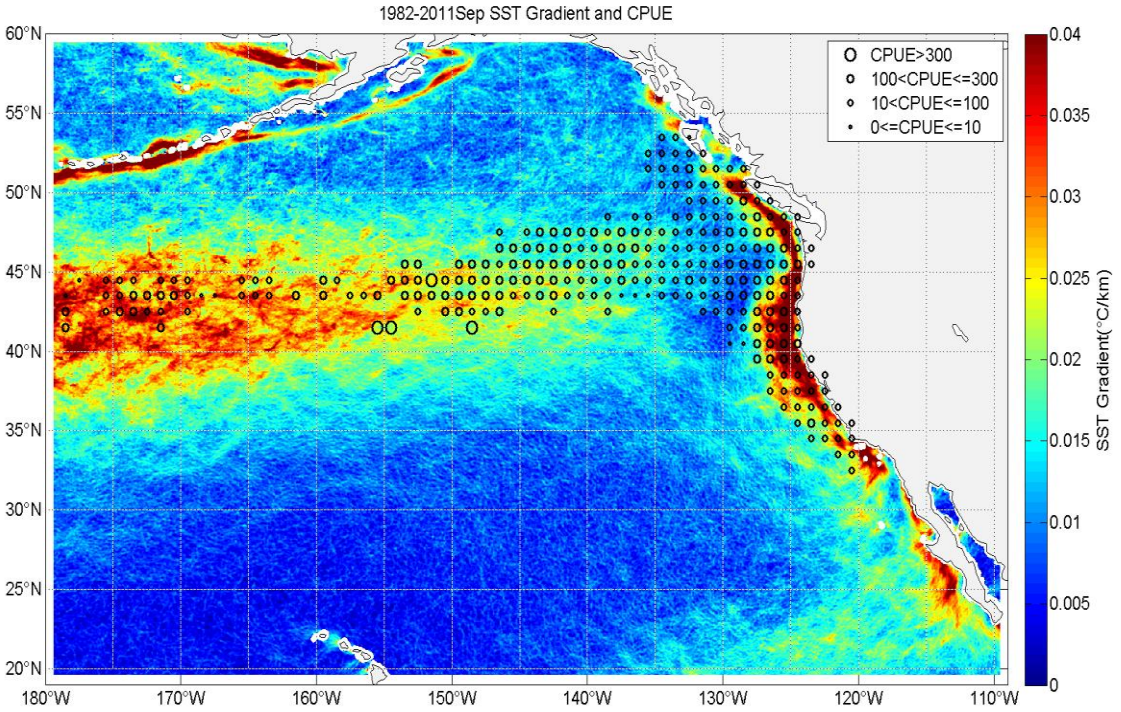


(f)

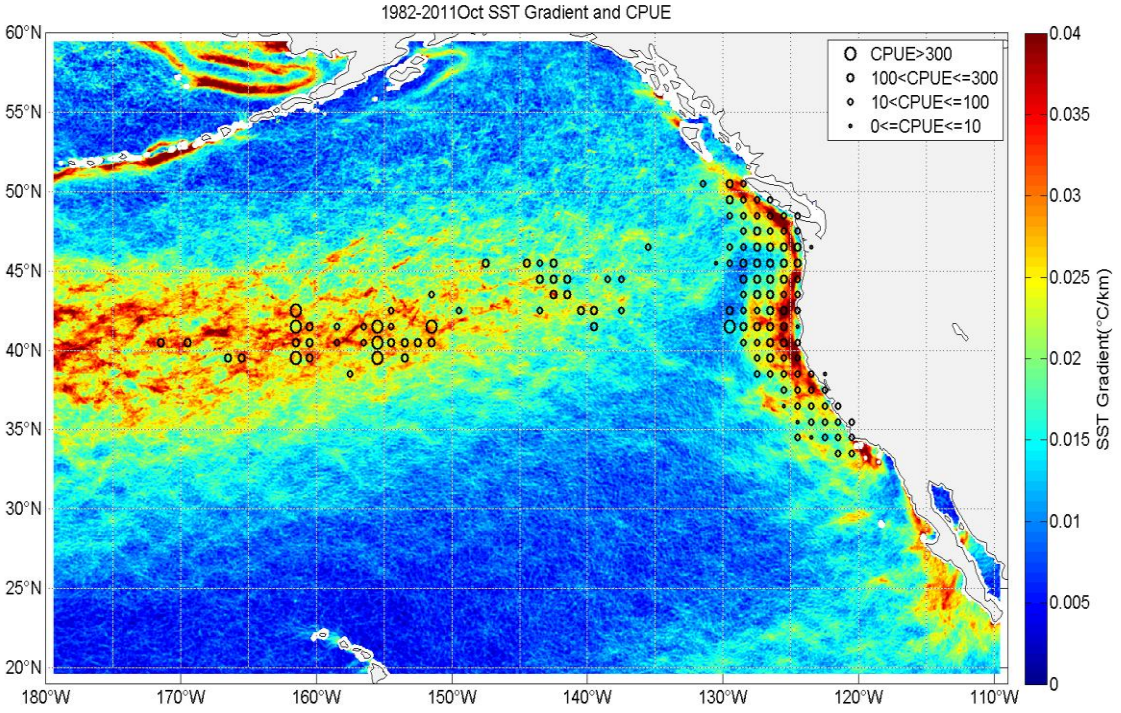


Figure S3. Continued.

(g)

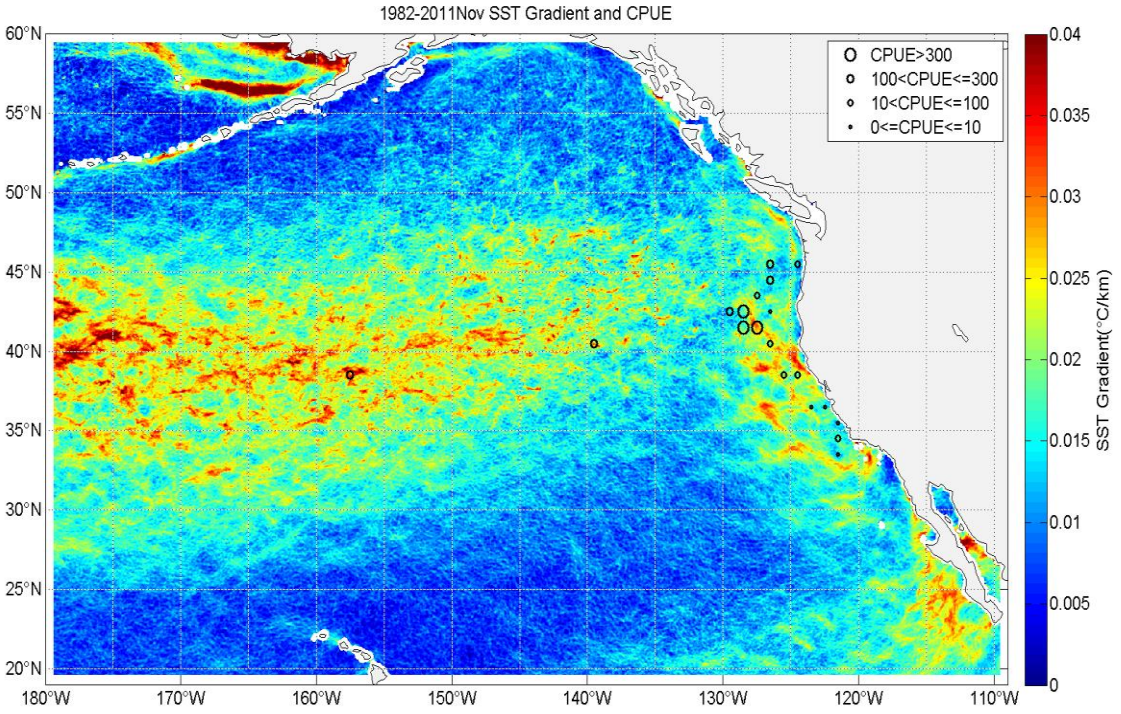


Figure S3. Continued.

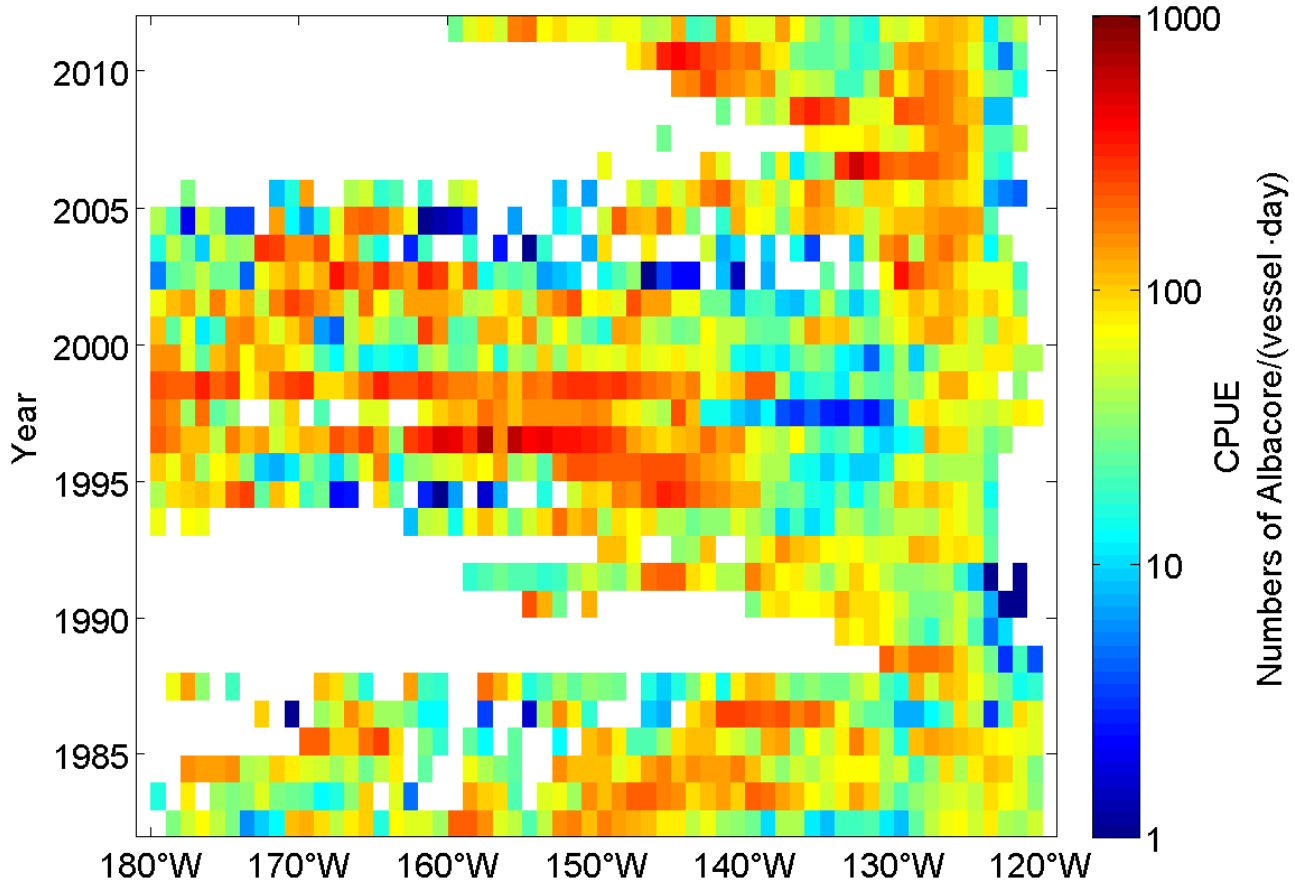


Figure S4. Interannual variation of longitudinal distribution of CPUE from 1982 to 2011. CPUE were averaged from 30 to 45°N. Strata with <=3 vessels were not shown due to data confidentiality requirements.

| Numbers of data under cloud (Total numbers of data 54,714) | | Window size | | |
|---|---|---|---|---|
| | | 3x3 pixels | 5x5 pixels | 7x7 pixels |
| % of cloud coverage | 100% | 3,619 | 2,469 | 1,653 |
| | More than 80% | 3,926 | 3,311 | 3,002 |
| | More than 60% | 4,823 | 4,347 | 4,278 |
| | More than 40% | 5,336 | 5,377 | 5,647 |

Table S1. The total numbers of fishing locations under the cloud. Different window size (3x3, 5x5 and 7x7) and different percentage of cloud coverage (100%, 80%, 60% and 40%) were chosen.

| Year | Numbers of data records in coastal area | Numbers of data records in open ocean | Proportion of data records in open ocean |
|---|---|---|---|
| 1982 | 3007 | 3329 | 0.5254 |
| 1983 | 3729 | 2194 | 0.3704 |
| 1984 | 4511 | 3094 | 0.4068 |
| 1985 | 3542 | 1796 | 0.3365 |
| 1986 | 1495 | 1963 | 0.5677 |
| 1987 | 2001 | 844 | 0.2967 |
| 1988 | 1885 | 154 | 0.0755 |
| 1989 | 1043 | 256 | 0.1971 |
| 1990 | 1849 | 1010 | 0.3533 |
| 1991 | 1028 | 1451 | 0.5853 |
| 1992 | 2766 | 1283 | 0.3169 |
| 1993 | 1777 | 1215 | 0.4061 |
| 1994 | 2335 | 2637 | 0.5304 |
| 1995 | 1614 | 4171 | 0.7210 |
| 1996 | 1640 | 4334 | 0.7255 |
| 1997 | 2413 | 4905 | 0.6703 |
| 1998 | 996 | 3040 | 0.7532 |
| 1999 | 3798 | 2696 | 0.4152 |
| 2000 | 3960 | 2229 | 0.3602 |
| 2001 | 4552 | 2606 | 0.3641 |
| 2002 | 3564 | 1435 | 0.2871 |
| 2003 | 3960 | 779 | 0.1644 |
| 2004 | 14097 | 772 | 0.0519 |
| 2005 | 16663 | 999 | 0.0566 |
| 2006 | 14605 | 1278 | 0.0805 |
| 2007 | 16585 | 193 | 0.0115 |
| 2008 | 12789 | 1326 | 0.0939 |
| 2009 | 17304 | 713 | 0.0396 |
| 2010 | 15708 | 2113 | 0.1186 |
| 2011 | 17968 | 892 | 0.0473 |

Table S2. Total numbers of data records in the coastal area (within 200 nautical miles of North American coast), the open ocean, and the proportion of the open ocean data records in the open ocean from 1982 to 2011.